Machine learning for pacemaker implantation prediction after TAVI using multimodal imaging data

Amine El Ouahidi, Yassine El Ouahidi, Pierre-Philippe Nicol, Sinda Hannachi, Clément Benic, Jacques Mansourati, Bastien Pasdeloup, Romain Didier

scientific reports

Check for updates

OPEN

Machine learning for pacemaker implantation prediction after TAVI using multimodal imaging data

Amine El Ouahidi[1]✉, Yassine El Ouahidi[2], Pierre-Philippe Nicol[1], Sinda Hannachi[1], Clément Benic[1], Jacques Mansourati[1], Bastien Pasdeloup[2] & Romain Didier[1]

Pacemaker implantation (PMI) after transcatheter aortic valve implantation (TAVI) is a common complication. While computed tomography (CT) scan data are known predictors of PMI, no machine learning (ML) model integrating CT with clinical, ECG, and transthoracic echocardiography (TTE) data has been proposed. This study investigates the contribution of ML methods to predict PMI after TAVI, with a focus on the role of CT imaging data. A retrospective analysis was conducted on a cohort of 520 patients who underwent TAVI. Recursive feature elimination with SHAP values was used to select key variables from clinical, ECG, TTE, and CT data. Six ML models, including Support Vector Machines (SVM), were trained using these selected variables. The model's performance was evaluated using AUC-ROC, F1 score, and accuracy metrics. The PMI rate was 18.8%. The best-performing model achieved an AUC-ROC of 92.1% ± 4.7, an F1 score of 71.8% ± 9.9, and an accuracy of 87.9% ± 4.7 using 22 variables, 9 of which were CT-based. Membranous septum measurements and their dynamic variations were critical predictors. Our ML model provides robust PMI predictions, enabling personalized risk assessments. The model is implemented online for broad clinical use.

Keywords ML, TAVI, Pacemaker, CT-Scan, Risk prediction, Membranous septum length

Abbreviations

ECG	Electrocardiogram
LCC	Left Coronary Cusp
ML	Machine Learning
CT	Computed tomography
MSL	Membranous septal length
NCC	Non-Coronary Cusp
PMI	Pacemaker implantation
SVM	Support Vector Machines
RCC	Right Coronary Cusp
TAVI	Transcatheter Aortic Valve Implantation
TTE	Transthoracic echocardiography

Motivation

Transcatheter aortic valve implantation (TAVI) is now the first line treatment of severe symptomatic aortic stenosis in case of suitable anatomies[1,2]. This stepwise validation towards lower surgical risk has been made possible by improved implantation techniques and systems with a reduced incidence of complications. Among these complications, the conductive disorders requiring implantation of a permanent pacemaker remain common and do not decrease significantly over time[3].

Moreover, pacemaker implantation (PMI) can have several potentially harmful effects: complications associated with pacemaker implantation (infection, bleeding from the pacemaker pocket), longer hospital stays, pacing-induced cardiomyopathy development leading to heart failure[4]. Identifying patients at risk for these complications is critical for improving patient outcomes.

Several clinical and electrical risk factors for conduction disturbances after TAVI have been identified, including male sex, first-degree AV block, and right bundle branch block[5]. Thanks to computed tomography (CT) imaging data, anatomical factors due to the anatomical relationship between the conduction pathways and the positioning of the new prosthesis have also been identified, such as short membranous interventricular

[1]Department of Cardiology, University Hospital of Brest, 29609 Bd Tanguy Prigent, Brest 29609, France. [2]IMT Atlantique Lab-STICC UMR CNRS, Brest 6285, France. ✉email: elouahidi.amine@gmail.com

septum, degree of aortic valve calcification and implantation depth[6,7]. Based on these anatomical data, new "recommendations" from valve manufacturers have been developed, including higher implantation with the "radiolucent method" and the "cusp overlap technique"[8,9]. However, this high implantation may be accompanied by an increase in other types of complications such as migration or embolization of the prosthesis, stroke, or coronary obstruction and compromise future coronary access.

Predicting accurately patients at risk of conductive disorders leading to PMI after TAVI is still a challenge to ensure effective management of the patient through the TAVI process: before, during and after the TAVI procedure.

Recent developments in machine learning (ML) provide a promising solution to this challenge. ML algorithms, which can learn from vast amounts of data and identify complex patterns, have the potential to improve predictive accuracy by incorporating a broader range of variables into the decision-making process[10]. While recent studies have used ML to predict PMI after TAVI, they have primarily focused on demographic, clinical, electrocardiographic (ECG), and transthoracic echocardiography (TTE) data, with limited use of CT-scan data[11–14]. Importantly, none of these studies have fully explored the contribution of CT imaging data—particularly variables such as membranous septum length and its variations—alongside other clinical variables in an integrated predictive model.

Given the critical need for more accurate predictive models and the promise of ML, our study is motivated by the goal of developing a comprehensive ML model that includes CT imaging data to improve the prediction of PMI risk post-TAVI. By better identifying at-risk patients, we can enhance preoperative planning and postoperative care, ultimately reducing the incidence of PMI and improving patient outcomes.

Contribution

This study aims to enhance PMI prediction after TAVI by incorporating pre-procedural CT imaging into a machine learning (ML) model. While previous models focused on clinical, ECG, and TTE data, we highlight the significant contribution of CT imaging, especially membranous septum measurements, to improving accuracy. Our key contributions include: (i) developing the first ML model to integrate clinical, ECG, TTE, and CT data for PMI prediction, showing performance gains with the inclusion of CT; (ii) introducing the novel use of diastolic membranous septum measurements and their interaction with systolic measurements (ΔdsMS) to assess PMI risk; and (iii) creating an online tool that provides personalized PMI risk estimates for clinicians, enhancing patient management. These innovations advance the field of PMI prediction by offering more comprehensive, accurate, and practical tools for improving patient outcomes after TAVI.

Methods

Context

Study population

This single-center retrospective study included consecutive patients who underwent TAVI at University Hospitals of Brest between January 2019 and December 2021. All patients were evaluated pre-TAVI by a multidisciplinary heart team, which used CT imaging to guide decisions on valve type, sizing, and vascular access. Post-operative PMI decisions were made by a cardiology team, including an electrophysiologist and an interventional cardiologist, following current guidelines[15].

The protocol was approved by the local Ethic Committee of the University Hospital of Brest (29BRC22.0127) and conducted in accordance with the Declaration of Helsinki. Patients provided informed consent for data use.

After excluding 69 patients with pre-existing pacemakers or defibrillators, 20 with poor-quality CT images, and 6 who died within 24 h post-TAVI, 520 patients remained for analysis. Of these, 18.8% received a pacemaker within 28 days. Detailed PMI indications are listed in (Table 1S).

Endpoints

The primary endpoint is to predict the risk of pacemaker implantation (PMI) within 28 days following TAVI. Our secondary objectives are: (1) To evaluate the relative importance of CT imaging variables, in relation to the others (Clinical, ECG, TTE) in predicting PMI risk; (2) To compare our post-TAVI model performance with a model using only pre-TAVI (data obtained during the preoperative evaluation) and per-TAVI (data obtained during the procedure in addition to pre-TAVI data) to assess their impact on prediction.

CT data

For all patients, an ECG-gated CT scan was performed as part of the pre-TAVI assessment, following standardized protocols[16]. The specific CT parameters studied are detailed in (Method. 1S). Key measurements were taken after identifying the virtual aortic basal ring using double-oblique views. These included: annular diameter (maximum and minimum, in mm), annular area in systolic and diastolic phases (mm^2), and the degree of calcification for each valvular cusp (LCC: Left Coronary Cusp, NCC: Non-Coronary Cusp, RCC: Right Coronary Cusp), visually graded as none, mild, moderate, or severe. The calcium score was calculated using the Agatston method[17] by contouring the valve calcifications at the annulus plane. We also noted the presence or absence of calcification in the upper interventricular septum and left ventricular outflow tract (LVOT). Additionally, membranous septal length (MSL) was measured in both systolic and diastolic phases, defined as the distance from the base of the aortic valve to the top of the muscular septum, using the modified coronal view as described by Hamdan et al.[6].

Variables of the dataset

We collected a total of 67 variables for analysis. These included 44 preprocedural variables: 20 from medical history, 6 electrical variables (ECG taken the day before TAVI), 6 from TTE (within 7 days before TAVI), and 12 from CT scans (performed within 6 months as part of procedural planning) (Table 1). Additionally, we gathered

Features	All ($n=520$)	Pacemaker ($n=98$)	No Pacemaker ($n=422$)	p-value
Age (years)	84,3 ± 5,5	84,7 ± 5,9	84,2 ± 5,4	0,25
Women	48,2% (251)	35,7% (35)	51,2%(216)	0,04
BMI (kg/m²)	26,5 ± 4,7	26,7 ± 5,4	26,4 ± 4,6	0,94
Clinical data				
Prior surgical aortic bioprosthesis	4,4% (23)	0,0% (0)	5,4% (23)	0,02
Prior CABG	6,5% (34)	7,1% (7)	6,4% (27)	0,966
Prior PCI	19,2% (100)	19,3% (19)	19,1% (81)	0,968
Prior peripheral arterial disease	8,6% (45)	8,1% (8)	8,7% (37)	0,854
Mellitus diabetes	17,6% (92)	16,3% (16)	18% (76)	0,721
Chronic respiratory failure	5,0% (26)	6,1% (6)	4,7% (20)	0,581
Previous stroke	7,3% (38)	11,2% (11)	6,4% (27)	0,111
Chronic kidney disease				0,004
stage 3	51,7% (269)	50% (49)	52,1% (220)	
stage 4	4,8% (25)	5,1% (5)	4,7% (20)	
stage 5	0,6% (3)	3,1% (3)	0,0% (0)	
Creatinine	90,2 ± 41	103 ± 72,1	87,1 ± 30,4	0,022
Logistic euroSCORE	9,5 ± 7,7	9,3 ± 7,5	9,6 ± 7,8	0,793
Acute coronary syndrome < 100days	1,3% (7)	1% (1)	1,4% (6)	0,657
Dyspnea NYHA 3 or 4	37,8% (197)	42,9% (42)	36,7% (155)	0,757
Syncope in the past year	3,6% (19)	11,2% (11)	1,9% (8)	< 0,001
Angina CCS 3 or 4	0,3% (2)	0,0% (0)	0,5% (2)	0,495
Anticoagulant therapy	27,3% (142)	32,6% (32)	26,0% (110)	0,26
Electrocardiogram data:				
Atrial fibrillation/flutter	20,1% (105)	19,4% (19)	20,4% (86)	0,844
PR time interval (ms)	186 ± 38	205 ± 48	181 ± 34	< 0,001
QRS time interval (ms)	104 ± 22	114 ± 24	102 ± 21	< 0,001
First degree AV block	73,6% (383)	56,1% (55)	77,7% (328)	0,024
Right bundle branch block	10,6% (55)	25,5% (25)	7,1% (30)	< 0,001
Left bundle branch block	9,6% (50)	8,1% (8)	9,9% (42)	0,606
TTE data:				
LVEF (%)	55,7 ± 10	55 ± 10	55,8 ± 10,3	0,256
Aortic valve systolic area	0,71 ± 0,2	0,73 ± 0,2	0,71 ± 0,2	0,107
Aortic valve systolic mean gradient	51 ± 20	51 ± 9	51 ± 2	0,283
sPAP (mmhg)	40 ± 13	39 ± 14	41 ± 13	0,117
Aortic regurgitation				0.559
I	34,8% (181)	39,8% (39)	33,6% (142)	
II	7,5% (39)	7,1% (7)	7,6% (32)	
III	1,3% (7)	2,1% (2)	1,2% (5)	
IV	1,5% (8)	0% (0)	1,9% (8)	
Mitral regurgitation				0.370
I	28,1% (146)	22,4% (22)	29,3% (124)	
II	8,6% (45)	6,1% (6)	9,2% (39)	
III	0,9% (5)	1% (1)	0,9% (4)	
IV	0,5% (3)	0,0% (0)	0,7% (3)	
CT data				
Minimal aortic annulus diameter (mm)	21,2 ± 2,25	21,5 ± 2,2	21 ± 2,2	0,045
Maximal aortic annulus diameter (mm)	26,1 ± 2,68	26,8 ± 2,6	25,9 ± 2,6	0,003
Systolic area (mm²)	482,6 ± 84	507,4 ± 89,2	476,5 ± 82,1	0,003
Diastolic area (mm²)	480,1 ± 88,6	504,8 ± 89,7	474,3 ± 87,5	0,004
Aortic calcium score	3789,7 ± 2021	4530,65 ± 2544	3606,8 ± 1827	0,001
LCC calcification				0,02
0	2,1% (11)	1,0% (1)	2,3% (10)	
1	65,1% (339)	63,2% (62)	65,6% (277)	
2	24,6% (128)	29,5% (29)	23,4% (99)	
3	3% (16)	6,1% (6)	2,3% (10)	
RCC calcification				0,003
Continued				

Features	All ($n=520$)	Pacemaker ($n=98$)	No Pacemaker ($n=422$)	p-value
0	2,6% (14)	1% (1)	3% (13)	
1	73,6% (383)	72,45% (71)	73,93% (312)	
2	15,77% (82)	19,39% (19)	14,93% (63)	
3	2,69% (14)	7,14% (7)	1,66% (7)	
NCC calcification				0,002
0	0,19% (1)	0,0% (0)	0,24% (1)	
1	46,1% (240)	35,7% (35)	48,5% (205)	
2	40,3% (210)	51% (50)	37,9% (160)	
3	8,1% (42)	13,3% (13)	6,9% (29)	
Calcium in basal septum				0,024
0	84,2% (438)	75,5% (74)	86,2% (364)	
1	15,6% (81)	24,5% (24)	13,5% (57)	
Calcium in LVOT				0,21
0	69,2% (360)	62,2% (61)	70,8% (299)	
1	30,5% (159)	37,7% (37)	28,9% (122)	
MSL (mm)				
diastole (dMSL)	$8,7 \pm 2,44$	$7,3 \pm 1,98$	$9,3 \pm 2,06$	$<0,001$
systole (sMSL)	$8 \pm 2,01$	$6,3 \pm 2,16$	$8,2 \pm 1,99$	$<0,001$
ΔdsMSL	$0,8 \pm 2,3$	$0,9 \pm 1,7$	$1,1 \pm 2,3$	$<0,001$
Aortic arch calcification	6,3% (33)	6,1% (6)	6,4% (27)	0,922

Table 1. Baseline characteristics of the overall population included. Values are n (%) or mean ± SD. *Abbreviations:AV: Atrioventricular*, *BMI: body mass index*, *CCS: Canadian Cardiovascular Society (Angina Grade)*, *ECG: Electrocardiogram*, *PCI: percutaneous coronary intervention*, *CABG: coronary artery bypass grafting*, *LCC: Left Coronary Cusp*, *LVEF: left ventricular ejection fraction*, *LVOT: Left ventricular outflow track*, *CT: computed tomography*, *MSL: Membranous septal length*, *NCC: Non-Coronary Cusp*, *NYHA: New-York Heart Association (heart failure functional classification)*, *RCC: Right Coronary Cusp*, *sPAP: systolic pulmonary arterial pressure*, *TTE: transthoracic echocardiograph*, *ΔdsMSL: difference between MSL in diastolic phase and in systolic phase measurements (dMSL-sMSL)*.

12 procedural variables (Table 2) and 11 postprocedural variables: 5 from ECG (within 3 h after TAVI) and 6 from TTE (within 6 h post-procedure) (Table 3). All CT measurements were taken prospectively and blinded to the prediction target (post-TAVI PMI), while the remaining variables were retrospectively extracted from medical records.

Statistical analysis

Patient characteristics were divided into two groups based on the presence or absence of PMI after TAVI. Group differences were assessed using the Mann-Whitney-Wilcoxon test for continuous variables and the Chi-Square test for categorical variables, with a significance threshold of $p<0.05$. Continuous variables are reported as mean ± standard deviation, or median (interquartile range) for non-normally distributed data. Categorical variables are shown as frequency and percentage (n, %). Statistical analyses were performed using Python 3.10.12 (Python Software Foundation) with the scipy stats module (v1.11.2). The performance of ML models in predicting PMI was evaluated using AUC-ROC, AUC-PR, accuracy, and F1-score metrics (Method. 2 S).

Preprocessing

Features engineering

To enhance model performance, we engineered new variables by combining combining two or more variables of the dataset, that we assumed pertinent in relation to the endpoints. These include: ΔPR and ΔQRS: difference between the baseline and first post-operative PR and QRS interval values, respectively; ΔsMSID: difference between sMSL (Membranous septal length in systolic phase) and ID (implantation depth) (MSL-ID); ΔdsMSL: difference between MSL in diastolic phase and in systolic phase measurements (dMSL-sMSL); Risk Zone Calcification (0 to 7) = RCC calcification grade (0 to 3) + NCC Calcification grade (0 to 3) + Interventricular septum Calcification (0 or 1); AVA ratio: ratio between the pre-TAVI TTE measurement of the aortic valve area and its post-TAVI area. *pre*AVA-PNA ratio: ratio between the pre-TAVI TTE measurement of the aortic valve area and the nominal surface area of the prosthesis given by the manufacturer; *post*AVA-PN ratio: ratio between the post-TAVI TTE measurement of the aortic valve area and the nominal surface area of the prosthesis given by the manufacturer.

Then, we transformed the categorical variables using one-hot encoding. After this step, we had a number of 204 variables.

Features	All ($n=520$)	Pacemaker ($n=98$)	No Pacemaker ($n=422$)	p-value
Annulus diameter used for TAVI selection	23,1 ± 2,36	23,8 ± 2,13	22,9 ± 2,39	0,001
Access site				0,702
transfemoral	93,1% (484)	91,8% (90)	93,3% (394)	
transaortique	0,9% (5)	1% (1)	0,9% (4)	
transapical	0,6% (3)	0,0% (0)	0,7% (3)	
carotid	5,4% (28)	7,1% (7)	4,9% (21)	
Procedure location				0,729
catheterization lab	88,4% (460)	85,7% (84)	89,1% (376)	
hybrid catheterization lab	4,6% (24)	6,1% (6)	4,2% (18)	
cardiac surgery operating room	6,7% (35)	8,1% (8)	6,4% (27)	
Valve size (mm)				0,004
23	20,2% (105)	14,3% (14)	21,5% (91)	
25	4,8% (25)	1% (1)	5,7% (24)	
26	34,2% (178)	30,6% (30)	35,1% (148)	
27	4% (21)	2% (2)	4,5% (19)	
29	30,2% (157)	39,8% (39)	27,9% (118)	
34	6,5% (34)	12,2% (12)	5,2% (22)	
Device type				0,067
EDWARS Sapien III	53,8% (280)	55,1% (54)	53,5% (226)	
COREVALVE	36,3% (189)	41,8% (41)	35,0% (148)	
evolut R	15,9% (83)	23,4% (23)	14,2% (60)	
evolut pro	20,3% (106)	18,3% (18)	20,8% (88)	
ACURATE	8,6% (45)	2% (2)	10,1% (43)	
Neo S	0,9% (5)	0,0% (0)	1,2% (5)	
Neo M	4% (21)	1% (1)	4,7% (20)	
Neo L	3,6% (19)	1% (1)	4,3% (18)	
PORTICO	1% (6)	1% (1)	1,2% (5)	
Transcatheter heart valve nominal area (mm^2)	490,5 ± 100,3	516,1 ± 99,1	484,6 ± 99,6	0,013
Area oversizing (%)	3,2 ± 9	1,5 ± 10	3,6 ± 9	0,150
Pre-dilatation	48,3% (251)	46,9% (46)	48,6% (205)	0,833
Post-dilatation	3,8% (20)	4,1% (4)	3,8% (16)	0,895
ID	5,3 ± 2,9	6,3 ± 3,1	5 ± 2,9	< 0,001
ΔMSID (MS systole)	2,8 ± 3,6	0,1 ± 3,7	3,2 ± 3,4	< 0,001

Table 2. Intraprocedural features. Values are n (%) or mean ± SD. *Abbreviations*: *ID: implantation depth*, *ΔsMSID: difference between sMSL(Membranous septal length in systolic phase) and implantation depth (sMSL-ID)*.

Preliminary feature selection

From this new set of variables, we made a primary selection phase to reduce their number. A random variable (X) from a normal distribution was introduced, and PMI was predicted using 204 variables plus X with models such as Random Forest (RF), Support Vector Machines (SVM), and Logistic Regression (LR) (Method. 3 S). Based on the prediction, each variable was ranked using the SHapley Additive exPlanations (SHAP) method, complemented by the Minimum Redundancy Maximum Relevance (MRMR) method[18, 19]. The rankings were averaged, and variables with less relevance than X ± 10% were removed, reducing the features by approximately 80%. The remaining 46 variables were then evaluated by a cardiologist for clinical relevance and used in subsequent experiments.

Machine learning

Models

We explored eight widely used ML models: LR, Decision Tree (DT), RF, standard Gradient Boosting model (GB), Extreme Gradient Boosting (XGBoost), Gaussian Naïve Bayes (GNB), MultiLayer Perceptron (MLP), and SVM. Models are detailed in the Supplementary (Method. 3 S). To develop our model, we used the Python scikit-learn library (1.2.2).

Identification of the best data processing chain

Given the 46 most relevant variables identified previously, we were then interested in determining the best series of data processing operations and choice of model among the possible options. To do so, we performed an exhaustive analysis of the following elements to determine which ones were beneficial to classification: (1)

Features	All ($n=520$)	Pacemaker ($n=98$)	No Pacemaker ($n=422$)	p-value
Electrocardiogram				
Atrial fibrillation/flutter	23,3% (121)	22,4% (22)	23,4% (99)	0,852
PR time interval (ms)	194,5 ± 40,1	225,6 ± 50,4	189,3 ± 35,6	< 0,001
QRS time interval (ms)	121,5 ± 27,7	135,9 ± 29,1	119,0 ± 26,7	< 0,001
ΔPR (ms)	9,04 ± 24,9	13,7 ± 28,3	8,2 ± 24,3	0,066
ΔQRS (ms)	17,7 ± 23,05	25,1 ± 26,56	16,4 ± 22,14	0,015
Right bundle branch block	14,4% (75)	35,7% (35)	9,4% (40)	< 0,001
Left bundle branch block	37,8% (197)	41,8% (41)	36,9% (156)	0,480
TTE:				
LVEF (%)	58,8 ± 10,2	59,1 ± 9,4	58,7 ± 10,4	0,972
Aortic valve systolic area (cm^2)	1,8 ± 0,6	1,9 ± 0,6	1,8 ± 0,6	0,154
AVA ratio	0,4 ± 0,2	0,4 ± 0,1	0,4 ± 0,2	0,589
Aortic Valve Systolic Mean Gradient	10,9 ± 4,7	10,8 ± 4,6	11 ± 4,7	0,995
Pulmonary artery pressure	39,4 ± 10,8	40,0 ± 12,3	39,31 ± 10,5	0,914
Aortic regurgitation (AR)				0,37
I	28,1% (146)	22,4% (22)	29,4% (124)	
II	8,6% (45)	6,1% (6)	9,2% (39)	
III	0,9% (5)	1% (1)	0,9% (4)	
IV	0,6% (3)	0,0% (0)	0,7% (3)	
Regurgitation localization				0,835
Peri-prosthetic AR	34,8% (181)	36,7% (36)	34,3% (145)	
Central-prosthetic AR	0,1% (1)	0,0% (0)	0,2% (1)	
Peri and central-prosthetic AR	0,4% (2)	0,0% (0)	0,5% (2)	
Mitral regurgitation				0,455
I	26,5% (138)	20,4% (20)	27,9% (118)	
II	6,5% (34)	5,1% (5)	6,9% (29)	
III	0,3% (2)	0,0% (0)	0,4% (2)	
IV	0,6% (3)	0,0% (0)	0,7% (3)	

Table 3. Post-procedural features. Values are n (%) or mean ± SD. *Abbreviations*: *AVA ratio: pre- to post-procedural ratio of AVA (pre/post)*, *LVEF: left ventricular ejection fraction*, *TTE: transthoracic echocardiography*, *ΔPR: difference between the baseline PR and first post-operative PR time*, *ΔQRS: difference between the baseline QRS and first post-operative QRS time*.

Handling outliers: options were clipping outliers identified with Z-score or none (no clipping); (2) Missing data: options for imputation were by mean, median, mode (most frequent value) or k nearest neighbors (kNN); (3) Normalization: options were standardization, MinMax or none; (4) Resampling: options were ROS (Random OverSampling), SMOTE (Synthetic minority oversampling technique) or none; (5) Model choice: options were all models described above.

For all configurations, a nested cross-validation (see below) was performed. At the end of this stage, we identified the best-performing model and its associated data processing sequence.

Model training procedure

In ML, it is common to partition the dataset into two disjoint sets: the train set and the test set. The test set is used to simulate an external test cohort, and the train set is used to train the model. The objective of any ML model is to learn (on the train set) to generalize to unseen (test set) data, to provide useful tools for prediction. To circumvent the limits of a single split, a common approach is to use nested cross-validation, i.e., cross-validation and cross-testing (Fig. 1S): 1) Cross-validation consists in splitting the train set into folds (10 here), 9 of which are used to train the model, and 1 (validation fold) to evaluate its generalization performance. For each choice of a validation fold, we independently train a model. We then keep the model hyperparameters that maximize average generalization performance of all these 10 models. Finally, we train a single model with these parameters on the entire train set, with the aim to maximize generalization ability of the model; 2) Cross-testing consists in splitting the entire dataset into folds (10 here), and to use 9 as a train set and 1 as test set. Thus, 10 models are independently trained (for each choice of a fold for the test set) using cross-validation. This methodology allows reported averaged results to be robust to the choice of a train/test split, and to provide confidence intervals.

Final model building, with finer feature selection

The aim of this stage is to optimize the model identified as the best performer in the previous stage and to optimize it by keeping only the minimum number of variables necessary to obtain the best results. The aim is to

improve clinician readability and to increase the model's performance. In order to identify the most influential variables and their optimal number on the basis of the model's predictive performance, we carry out a second phase of "fine" selection in addition to the preliminary feature selection (see above). We opted to implement Recursive Feature Elimination (RFE), along with the SHAP method. When applied once, the model is trained on all the variables except the less relevant one identified with SHAP. This is done iteratively until the best performance is found. This approach enables the identification of the most influential variables and their optimal count based on the model's predictive performances.

The Synthetic view of the workflow for finding the best model and training pipeline for predicting PM implantation is available in Fig. 1.

Results

Model performances for the outcome of PMI within 28 days

Using the F1 score as a performance metric (relevant in our case because our prediction target prediction target is unbalanced, i.e., 18.8% PMI), the results were as follows (in decreasing order): SVM achieved 67.26% ± 9.72, LR 66.04% ± 9.79, MLP 62.66% ± 10.83, XGBoost 62.25% ± 13.1, GB 62.18% ± 13.91, RF 60.58% ± 13.34, GNB 58.8% ± 9.11, and DT 56.13% ± 13.03. The AUC-ROC and AUC-PR curves for all the models are shown in (Fig. 2A and B). **S**VM emerged as the top-performing model, closely followed by LR, with both models outperforming the rest.MLP, GB, XGBoost, RF performed similarly and were better than GNB and DT. Given its superior performance, SVM will be used in the subsequent sections to present additional ML results.

Variables used to generate predictions for our final model

By using the elements of the processing chain that led to the best performance of the SVM (ROS, imputation of missing values by the median, standardization) and by selecting the most relevant variables to generate the predictions, we obtained, after final training of the model, an AUC-ROC of 92.1% ± 4.7 and a PR-ROC of 77.6% ± 9.9.

SHAP variable selection allows us to study the 22 variables used by the model to generate these results: 8 CT-scan variables, 7 ECG variables, 2 TTE variables, 3 procedure-related variables and 2 clinical variables. The SHAP results are shown in Fig. 3A. Figure 3B shows the confusion matrix resulting from all the predictions made by our model. We obtain only 3.4% of false negatives (patients predicted by our model as not having been implanted with a pacemaker when they were in fact implanted) and 8.7% of false positives (patients predicted by our model as having been implanted when they were not).

Importance of CT imaging variables in predicting PMI risk

As observed above, CT-scan variables have a central place in the variables used to train the best model (8 variables out 22). To understand the importance of each modality (clinical, ECG, TTE, CT, procedure-related data) in a quantitative way, we performed another series of experiments by training the best-found model (SVM) using only data from a given modality. In Fig. 4, the results of these analyses confirm the central place of imaging data, in the forefront of which are CT-scan data. In fact, using only CT-scan data leads to excellent performance (87.7% ± 6.1 and 64.2 ± 9 according to AUC and F1-score respectively), which is close to the predictions using all the variables (92.1 ± 4.7 and 77.6 ± 9.9 according to AUC and F1-score respectively) determined to be important. In Fig. 2S. the variables selected by SHAP + RFE are given for each type of modality.

Pre, per and post-procedural prediction models

Results previously presented come from training the models on post-TAVI data (thus using all the pre + per + post variables). In this section, we also present the performance of the SVM using only the data acquired in the pre-TAVI, then adding the per-TAVI data (i.e., pre + per). The addition of per- and post- data resulted in a gain in performance compared to using the pre-TAVI data in isolation, as can be seen from the data in Table 2S (+ 2.4% and + 6.7% according to AUC and F1-score respectively).

Discussion

This retrospective study demonstrates the potential of machine learning (ML) methods, particularly a Support Vector Machine (SVM) architecture, in predicting pacemaker implantation (PMI) following transcatheter aortic valve implantation (TAVI). Our results show that incorporating a variety of data sources—clinical, electrocardiographic (ECG), transthoracic echocardiography (TTE), and computed tomography (CT) imaging—leads to significantly improved predictive performance. In particular, membranous septum parameters (dMSL, ΔsMSID, ΔdsMS) played a crucial role in enhancing the model's accuracy.

Contribution of artificial intelligence to high-performance prediction

This study illustrates the capability of ML models to improve clinical risk prediction for complex, multifactorial events such as PMI after TAVI. Unlike traditional predictive scores, which typically incorporate limited variables, our ML model integrates a broader range of data, including detailed anatomical information from CT scans, to provide a more comprehensive risk assessment. By employing rigorous methods such as nested cross-validation and advanced feature selection techniques, our model achieves a high level of predictive performance.

The place of our study in the current literature

Several studies have explored the use of machine learning (ML) models to predict the risk of pacemaker implantation (PMI) following TAVI. Four notable studies have highlighted the utility of ML models in this context. However, it is important to note that a direct comparison of our model's performance to these previous

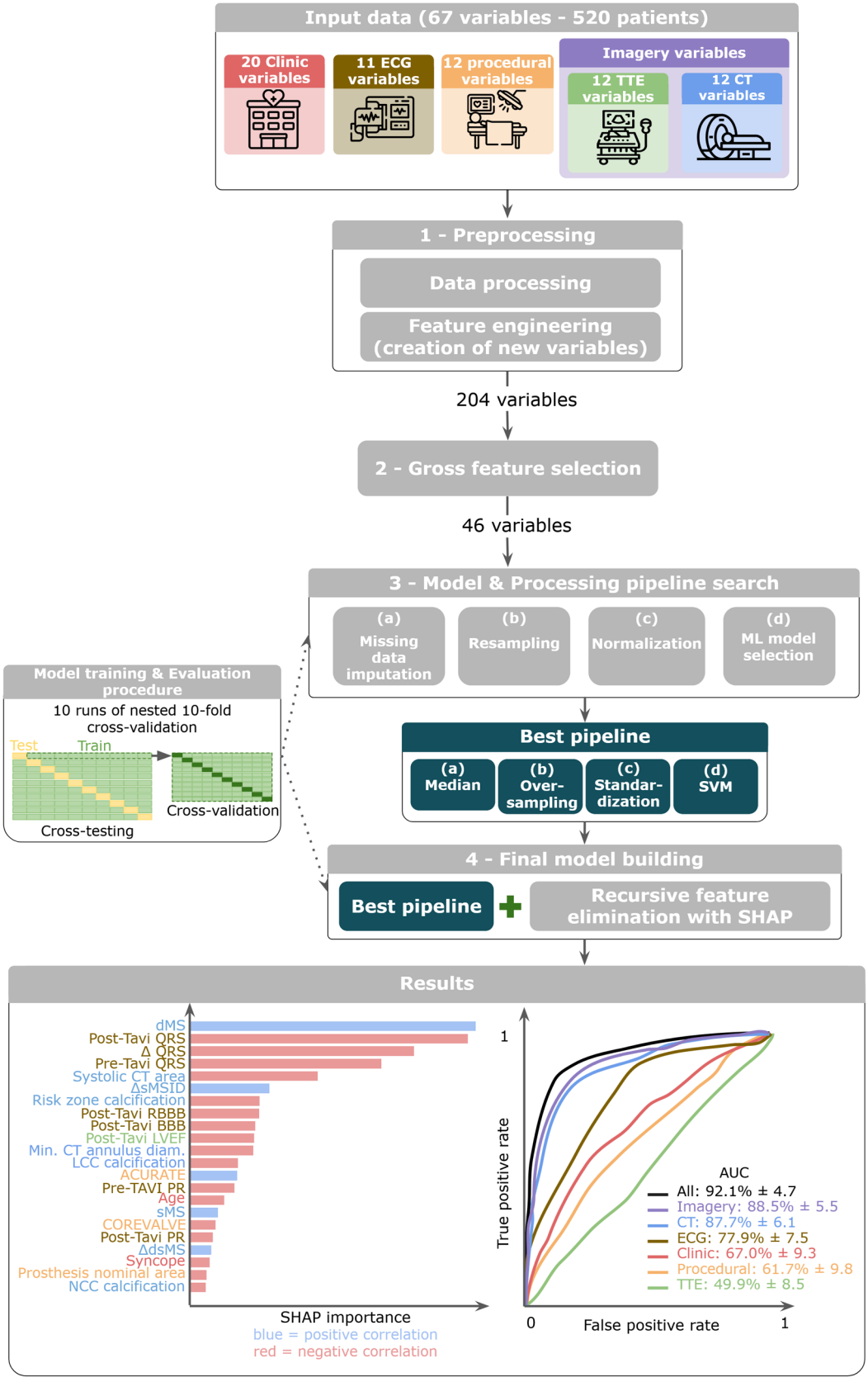

studies cannot be considered here. Ideally, a fair comparison would require testing all models on the same dataset, which was not possible in this case. (i) Gomes et al.[11] focused on predicting in-hospital mortality post-TAVI and also trained an ML model to predict PMI. Their model, using Support Vector Machines (SVM), achieved an AUC-ROC of 61% and an accuracy of 70%. (ii) Truong et al.[12] trained a random forest model on 557 patients using 38 features, achieving an AUC-ROC of 81%, an accuracy of 76%, and an F1 score of 49%.

◂**Fig. 1**. Synthetic view of the workflow for finding the best model and training pipeline for predicting PM implantation. The dataset consists of 520 patients, each with 67 variables of various modalities, identified with distinct colors. In step 1 (*Preprocessing*), we perform data processing and introduce new variables. This leads to 204 variables per patient, from which we determine the most significant ones in step 2 (*Gross feature selection*). After this selection, we have 46 variables left per patient. Using these, we enter step 3 (*Model & Processing pipeline search*), where we exhaustively define all the possible pipelines and models, trained with the nested cross-validation procedure (*Model training & Evaluation procedure*). Finally, in step 4 (*Final model building*), we take the best pipeline found, and proceed with a recursive feature elimination method using SHAP to reduce the number of variables. This leads to a final list of 22 variables that are most correlated with PM implantation. The model is then trained again with these variables using nested cross-validation again. The first figure (*Results*, *left*) details the remaining variables, with colors corresponding to those of input data. They are sorted in decreasing SHAP importance, and bar colors indicate a positive or negative correlation with PM implantation. The second figure (*Results*, *right*) shows the AUC-ROC curves obtained using the best pipeline, for all modalities, as well as for each modality taken individually.

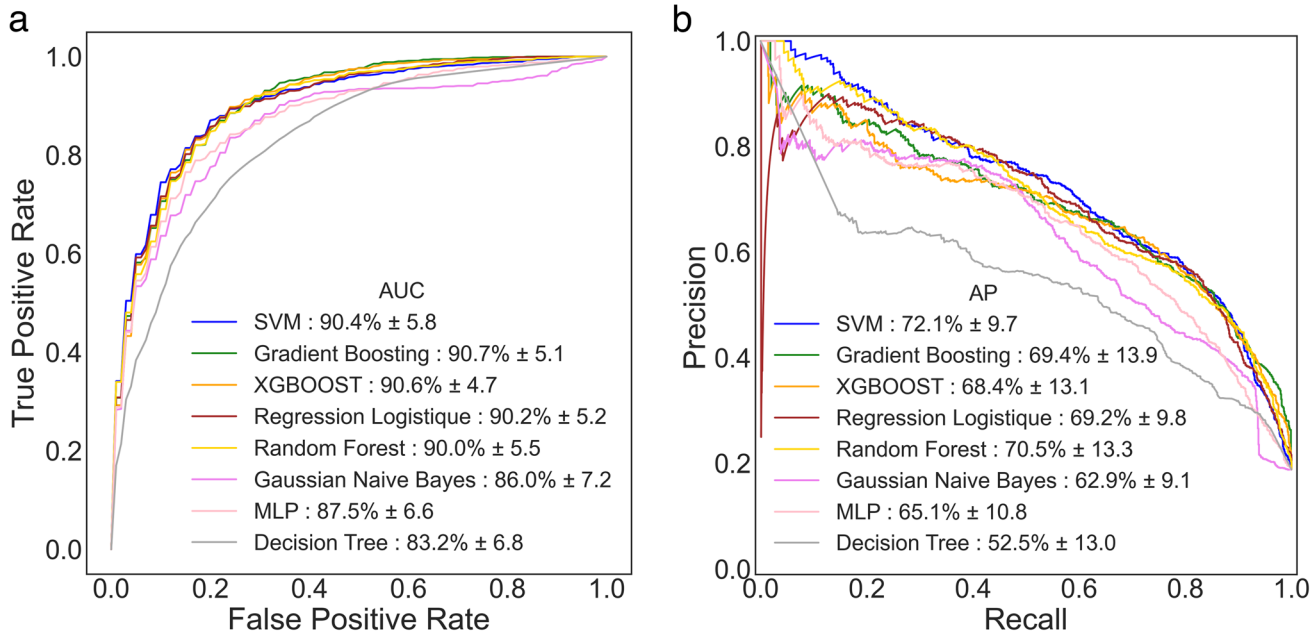

Fig. 2. (**A**) Model performances for the outcome of PMI within 28 days. AUC-ROC curves, (**B**) AUC-Precision-Recall Curves. *Abbreviations: XGBoost: Extreme Gradient Boosting (XGBoost), MLP: MultiLayer Perceptron, SVM: Support Vector Machine.*

(iii) Tsushima et al.[13] used a larger cohort of 1,390 patients and applied logistic regression and locally weighted learner-based classifiers. Their models reached the highest AUC-ROC of 82%, an accuracy of 68%, and F1 scores of 61% for SLR and 59% for LWL. (iv) Agasthi et al.[14] employed a Gradient Boosting Machine (GBM) model to predict PMI 30 days post-TAVR, with an AUC-ROC of 65%.

The first three studies primarily relied on clinical, electrical (ECG), echocardiographic (TTE), and procedural data, such as valve type and approach. While Agasthi et al. incorporated six CT variables in their model, none of these studies included critical anatomical features like membranous septum length (MSL) or implantation depth, which have been shown to significantly impact PMI risk. In contrast, our study integrates a wider range of variables, particularly from CT imaging, that were not considered in these previous studies. This inclusion of detailed anatomical data offers a more comprehensive predictive approach.

In addition to ML-based studies, Kiani et al. developed the Emory Risk Score (ERS) using a multivariate regression model to predict PMI after TAVI[15]. When we applied the ERS to our dataset, it resulted in an AUC-ROC of 62.3% ± 8.5, an F1 score of 35.8% ± 11.2, and an accuracy of 72.3% ± 5.2, further underscoring the superior performance of ML models (Fig. 3S).

Useful variables for performance improvement

Whether using pre-, per-, or post-TAVI data for prediction, all types of variables (clinical, ECG, TTE, and CT) consistently appeared among the selected features. To the best of our knowledge, no existing ML model has been developed that accurately predicts PMI after TAVI by integrating all of these variable types. Additionally, we demonstrated significant performance gains with the inclusion of CT data.

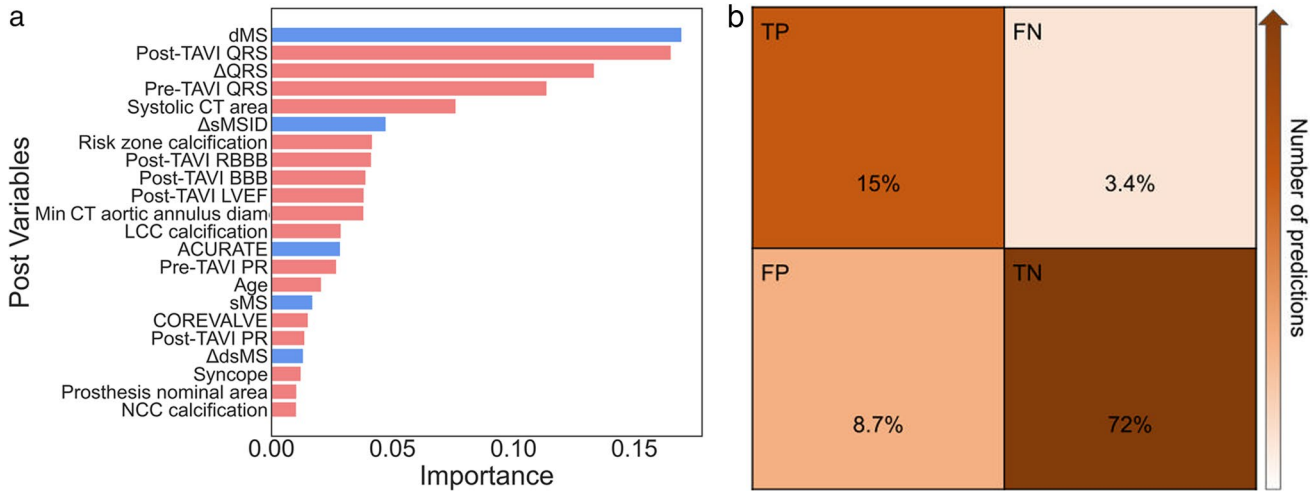

Fig. 3. (**A**) Feature importance from the SVM model. (**B**) Confusion matrix from the SVM model. *Abbreviations: dMSL: diastolic Membranous septal length, LVEF: left ventricular ejection fraction, dMSL: diastolic Membranous septal length, MR: Mitral regurgitation, NCC: Non-Coronary Cusp, NYHA: New-York Heart Association (heart failure functional classification), RCC: Right Coronary Cusp, sPAP: systolic pulmonary arterial pressure, TTE: transthoracic echocardiograph,ΔdsMSL: difference between MSL in diastolic phase and in systolic phase measurements (dMSL-sMSL);ΔQRS: difference between the baseline QRS and first post-operative QRS time.*

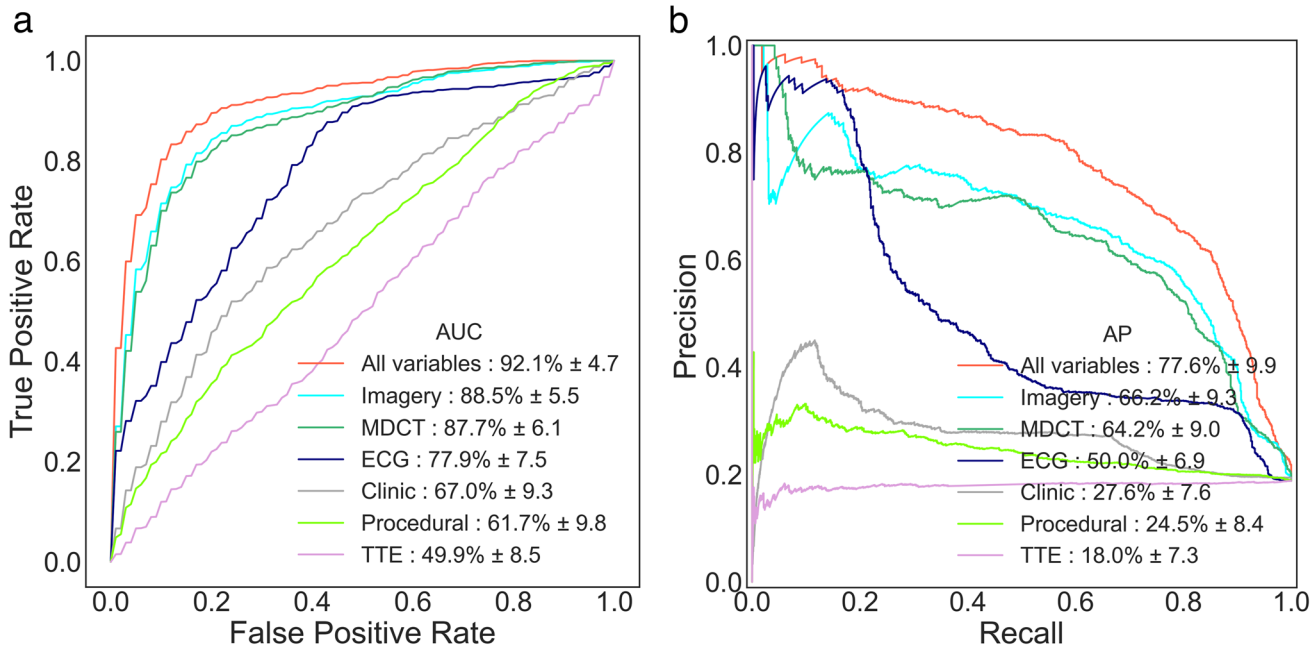

Fig. 4. Model performance according to the type of data used to predict PMI within 28 days. (**A**) AUC-ROC curves, (**B**) AUC-Precision-Recall Curves. *Abbreviations: TTE: transthoracic echocardiography, Imagery: CT+TTE.*

Furthermore, this is the first study to describe the diastolic membranous interventricular septum (MSL) measurement and its interaction with the systolic MSL, characterized by the ΔdsMS variable, in ML-based prediction. The membranous septum (MS) is a known anatomical landmark visible on CT, correlating with the location of the atrioventricular bundle and the left bundle branch. A meta-analysis of 18 studies, including 5,740 patients, confirmed that a shorter MS length and low (ΔsMSID) are associated with a higher risk of conduction disturbances[16]. While MSL is routinely measured in systole, we incorporated both diastolic MSL measurements and its variation throughout the cardiac cycle (ΔdsMS) into our dataset. Both variables were associated with improved prediction performance.

The ΔdsMS variable can be interpreted as a measure of MSL stiffness. A reduction in its value reflects decreased MSL deformability, which can result from MSL area calcification (including calcifications in the NCC/RCC and upper interventricular septum, all associated with PMI after TAVI). Additionally, low deformability could also occur in cases of infiltrative heart disease, such as TTR amyloidosis, which affects approximately 1 in 7 patients undergoing TAVI[17]. This increased stiffness may lead to greater MSL fragility, thereby increasing the risk of damage to the conduction pathway and, subsequently, the need for PMI.

Implementation of a practical tool

To assess the impact of pre-, per-, and post-TAVI data on model performance, we developed three separate models: one trained using only pre-TAVI data, another using both pre- and per-TAVI data, and a third incorporating all data (pre-, per-, and post-TAVI). These models are available through an online tool, which clinicians can use for real-time predictions. By inputting the required variables, clinicians can select the most appropriate model based on the stage of patient management (pre-, per-, or post-TAVI) and receive a personalized PMI risk percentage. Additionally, a public repository with the code for reproducing the experiments is available for further research or validation.

This user-friendly tool enables clinicians to estimate post-operative PMI risk more accurately, thereby improving patient care. A prospective study will be necessary to determine specific risk thresholds that could guide clinical decisions. In practice, a low predicted PMI risk may support early hospital discharge, while a higher risk would indicate the need for extended monitoring and closer surveillance.

Limitations

First, as this is a retrospective and single-center study, external validation is necessary to assess the reproducibility and generalizability of our prediction model to different patient populations. Second, the relatively high PMI rate (18%) may be partially attributed to the use of the three-cusp coplanar projection technique during the procedure, which is known to be more prone to conduction disturbances compared to the cusp overlap technique[18]. Third, due to the lack of clear guidelines regarding PMI after TAVI, there is often a discrepancy between the rate of pacemaker implantation and the rate of actual pacemaker usage. It is estimated that only one-third of patients use their pacemaker within one year of implantation. Similar to other studies, our model was developed to predict PMI based on this reality. Fourth, the low post-dilation rate in our database (3.8%) can be explained by our local practice, which aims to minimize post-dilatation after valve deployment to reduce potential risks, such as TAVI migration, conduction system trauma, rupture of the membranous septum or aorta, and cerebrovascular embolism. Finally, membranous septum length (MSL) can be measured using two different approaches: coronal MSL and infra-annular MSL, which may yield different results. Currently, there is no clear consensus on the preferred method, so we opted for the coronal MSL approach, as it aligns more closely with the angiographic view used to measure implantation depth (ID).

Translational outlook

Our model lays the groundwork for future research in post-TAVI complications. The same ML approach could be applied to predict other complications such as paravalvular leaks or stroke, enhancing preoperative risk stratification across multiple dimensions. Furthermore, integrating deep learning techniques to directly analyze CT-Scan DICOM images could eliminate manual feature extraction, potentially improving the accuracy of future predictive models[19,20].

Conclusion

This study demonstrates the potential of a machine learning (ML) model, particularly using a Support Vector Machine (SVM) architecture, to accurately predict the risk of pacemaker implantation (PMI) following transcatheter aortic valve implantation (TAVI). The significance of this research lies in its contribution to addressing a critical clinical challenge—reducing the incidence of PMI, which is associated with increased morbidity and healthcare costs.

A key finding is the substantial role of computed tomography (CT) imaging data, especially membranous septum length (MSL), in enhancing predictive accuracy. By integrating detailed CT imaging with other clinical variables, our model provides a more comprehensive approach to risk stratification, potentially leading to improved patient outcomes.

Additionally, we have developed an online tool based on our predictive model. This tool allows clinicians to input necessary variables and obtain a personalized PMI risk percentage, enabling more precise and informed clinical decision-making. Such a tool can be particularly valuable in optimizing patient management by guiding preoperative screening and post-operative care.

As TAVI indications continue to expand, the integration of artificial intelligence in clinical practice offers promising potential for improving patient care.

Looking forward, future research should focus on validating this model in larger, multicenter studies to confirm its generalizability. Using the same ML methods, there is potential to predict other post-TAVI complications, such as paravalvular leak or stroke. Additionally, a deep learning approach that directly incorporates CT-Scan DICOM images as input could yield promising results by eliminating the need for manual feature extraction and potentially improving predictive accuracy. We encourage ongoing exploration and development of AI-driven tools in cardiology, as they hold significant promise for advancing personalized medicine and enhancing patient outcomes.

Data availability

The datasets analyzed during the current study are available from the corresponding author on reasonable request. All the code used for preprocessing and model implementation is also available online: https://github.com/elouayas/predict_pm_tavi The model is implemented online for broad usage: https://huggingface.co/spaces/elouayas/pacemaker_implantation_TAVI.

Received: 20 July 2024; Accepted: 10 October 2024
Published online: 23 October 2024

References

1. Popma, J. J. et al. Transcatheter aortic-valve replacement with a self-expanding valve in low-risk patients. *N Engl. J. Med.* **380**, 1706–1715 (2019).
2. Mack, M. J. et al. Transcatheter aortic-valve replacement with a balloon-expandable valve in low-risk patients. *N Engl. J. Med.* **380**, 1695–1705 (2019).
3. Auffret, V. et al. Conduction disturbances after transcatheter aortic valve replacement: current status and future perspectives. *Circulation*. **136**, 1049–1069 (2017).
4. Sammour, Y. et al. Incidence, predictors, and implications of permanent pacemaker requirement after transcatheter aortic valve replacement. *JACC Cardiovasc. Interv*. **14**, 115–134 (2021).
5. Siontis, G. C. M. et al. Predictors of permanent pacemaker implantation in patients with severe aortic stenosis undergoing TAVR: a meta-analysis. *J. Am. Coll. Cardiol.* **64**, 129–140 (2014).
6. Hamdan, A. et al. Inverse relationship between membranous septal length and the risk of atrioventricular block in patients undergoing transcatheter aortic valve implantation. *JACC Cardiovasc. Interv*. **8**, 1218–1228 (2015).
7. Maier, O. et al. Computed tomography derived predictors of permanent pacemaker implantation after transcatheter aortic valve replacement: a meta-analysis. *Catheter Cardiovasc. Interv Off J. Soc. Card Angiogr Interv*. **98**, E897–E907 (2021).
8. Sammour, Y. et al. Systematic Approach to High Implantation of SAPIEN-3 Valve achieves a lower rate of conduction abnormalities including pacemaker implantation. *Circ. Cardiovasc. Interv*. **14**, e009407 (2021).
9. Tang, G. H. L. et al. Cusp-overlap' View simplifies fluoroscopy-guided implantation of self-expanding valve in transcatheter aortic valve replacement. *JACC Cardiovasc. Interv*. **11**, 1663–1665 (2018).
10. Quer, G., Arnaout, R., Henne, M. & Arnaout, R. Machine learning and the future of Cardiovascular Care: JACC State-of-the-art review. *J. Am. Coll. Cardiol.* **77**, 300–313 (2021).
11. Gomes, B. et al. Machine learning-based risk prediction of intrahospital clinical outcomes in patients undergoing TAVI. *Clin. Res. Cardiol. Off J. Ger. Card Soc.* **110**, 343–356 (2021).
12. Truong, V. T. et al. Machine learning method for predicting pacemaker implantation following transcatheter aortic valve replacement. *Pacing Clin. Electrophysiol. PACE*. **44**, 334–340 (2021).
13. Tsushima, T. et al. Machine learning algorithms for prediction of Permanent Pacemaker Implantation after Transcatheter aortic valve replacement. *Circ. Arrhythm. Electrophysiol.* **14**, e008941 (2021).
14. Agasthi, P. et al. Prediction of permanent pacemaker implantation after transcatheter aortic valve replacement: the role of machine learning. *World J. Cardiol.* **15**, 95–105 (2023).
15. Kiani, S. et al. Development of a risk score to Predict New Pacemaker Implantation after Transcatheter aortic valve replacement. *JACC Cardiovasc. Interv*. **12**, 2133–2142 (2019).
16. Sá, M. P. et al. Computed tomography-derived membranous septum length as predictor of conduction abnormalities and permanent pacemaker implantation after TAVI: a meta-analysis of observational studies. *Catheter Cardiovasc. Interv Off J. Soc. Card Angiogr Interv*. **101**, 1203–1213 (2023).
17. Castaño, A. et al. Unveiling transthyretin cardiac amyloidosis and its predictors among elderly patients with severe aortic stenosis undergoing transcatheter aortic valve replacement. *Eur. Heart J.* **38**, 2879–2887 (2017).
18. Sá, M. P. et al. Cusp-overlap versus coplanar view in transcatheter aortic valve implantation with self-expandable valves: a meta-analysis of comparative studies. *Catheter Cardiovasc. Interv Off J. Soc. Card Angiogr Interv*. **101**, 639–650 (2023).
19. Haq, I. et al. Lung nodules localization and report analysis from computerized tomography (CT) scan using a Novel Machine Learning Approach. *Appl. Sci.* **12**, 12614 (2022).
20. Chen, Y. et al. LDANet: automatic lung parenchyma segmentation from CT images. *Comput. Biol. Med.* **155**, 106659 (2023).

Author contributions

• AE: research conception, data collection, data analysis, modeling and writing of the manuscript; • YE: research conception, data analysis, modeling, online tool conception and writing of the manuscript; • RD and BP: research conception, data interpretation, critical revision of the manuscript. • All authors participated in the discussion of the concept of the study.

Funding

None.

Declarations

Competing interests

The authors declare no competing interests.

Additional information

Supplementary Information The online version contains supplementary material available at https://doi.org/10.1038/s41598-024-76128-z.

Correspondence and requests for materials should be addressed to A.E.O.